Available online at www.sciencedirect.com
SCIENCE DIRECT®
International Journal of Thermal Sciences 42 (2003) 605–619
International Journal of Thermal Sciences
www.elsevier.com/locate/ijts

# Integrated human-clothing system model for estimating the effect of walking on clothing insulation

Nesreen Ghaddar [a,*], Kamel Ghali [b], Byron Jones [c]

[a] *American University of Beirut, Faculty of Engineering and Architecture, P.O. Box 11-236, Riad ElSolh, Beirut 1107 2020, Lebanon*
[b] *Beirut Arab University, Faculty of Engineering, Beirut, Lebanon*
[c] *Kansas State University, College of Engineering, 148 Rathbone Hall, Manhattan, KS 66506-5202, USA*

Received 3 January 2002; accepted 3 September 2002

**Abstract**

The objective of this work is to develop a 1-D transient heat and mass transfer model of a walking clothed human to predict the dynamic clothing dry heat insulation values and vapor resistances. Developing an integrated model of human and clothing system under periodic ventilation requires estimation of the heat and mass transfer film coefficients at the skin to the air layer subject to oscillating normal flow. Experiments were conducted in an environmental chamber under controlled conditions of 25 °C and 50% relative humidity to measure the mass transfer coefficient at the skin to the air layer separating the wet skin and the fabric. A 1-D mathematical model is developed to simulate the dynamic thermal behavior of clothing and its interaction with the human thermoregulation system under walking conditions. A modification of Gagge's two-node model is used to simulate the human physiological regulatory responses. The human model is coupled to a clothing three-node model of the fabric that takes into consideration the adsorption of water vapor in the fibers during the periodic ventilation of the fabric by the air motion in from ambient environment and out from the air layer adjacent to the moist skin. When physical activity and ambient conditions are specified, the integrated model of human-clothing can predict the thermoregulatory responses of the body together with the temperature and insulation values of the fabric. The developed model is used to predict the periodic ventilation flow rate in and out of the fabric, the periodic fabric regain, the fabric temperature, the air layer temperature, the heat loss or gain from the skin, and dry and vapor resistances of the clothing. The heat loss from the skin increases with the increase of the frequency of ventilation and with the increased metabolic rate of the body. In addition, the dry resistance of the clothing fabrics, predicted by the current model, IS compared with published experimental data. The current model results compare qualitatively well with published data and show significant decrease in the clothing dry and evaporative insulation values.


*Keywords:* Periodic fabric ventilation; Dynamic human-clothing model; Heat and mass transfer; Trapped air layer

## 1. Introduction

Transport of heat and moisture from the human skin is initiated by gradients of temperature and moisture concentration of the air within the fabric, the air space between skin and fabric, and the ambient air. The transport processes are not only of diffusion type but also are enhanced by the ventilating motion of air through the fabric initiated by the relative motion of the human with respect to the surrounding environment. The size of the air spacing between the skin and the fabric is continuously varying in time depending on the level of activity and the location, thus inducing variable airflow in and out of the fabric. This induced airflow ventilates the fabric and contributes to the augmentation of the rate of condensation and adsorption in the clothing system and the amount of heat and moisture loss from the body. During body motion, air must go in and out and ventilation is obtained without gross environmental air movement. Harter et al. called this particular aspect in clothing comfort "ventilation of the microclimate within clothing" [1]. The ventilation rate is affected mainly by the walking velocity as described by Lotens, who derived empirically the steady ventilation rate through apertures of clothing assembly as function of the air permeability of the fabric and the effective wind velocity [2]. His model was derived from experimental considerations of forced convective flow through apertures of outer

* Corresponding author.
*E-mail addresses:* farah@aub.edu.lb (N. Ghaddar), amro@aub.edu.lb (K. Ghali), jones@ksu.edu (B. Jones).

1290-0729/03/$ – see front matter 
doi:10.1016/S1290-0729(03)00026-7

**Nomenclature**

| | | |
|---|---|---|
| $A$ | area of the fabric | $m^2$ |
| $C_{cr}$ | heat capacity of the human core node | $J{\cdot}K^{-1}$ |
| $C_f$ | fiber specific heat | $J{\cdot}kg^{-1}{\cdot}K^{-1}$ |
| $C_v$ | air specific heat at constant volume | $J{\cdot}kg^{-1}{\cdot}K^{-1}$ |
| $c_{bl}$ | specific heat of blood, = 4.187 | $kJ{\cdot}kg^{-1}{\cdot}K^{-1}$ |
| $C_{sk}$ | heat capacity of the human skin node | $J{\cdot}K^{-1}$ |
| $D$ | the mass diffusivity of water vapor into air | $m^2{\cdot}s^{-1}$ |
| $e$ | thickness | m |
| $f$ | frequency of oscillation | Hz |
| $h_{fg}$ | heat of vaporization of water | $J{\cdot}kg^{-1}$ |
| $h_{ad}$ | heat of adsorption | $J{\cdot}kg^{-1}$ |
| $H_{ci}$ | conduction heat transfer coefficient between inner node and outer node | $W{\cdot}m^{-2}{\cdot}K^{-1}$ |
| $H_{co}$ | convection heat transfer coefficient between outer node and air flowing through fabric | $W{\cdot}m^{-2}{\cdot}K^{-1}$ |
| $h_{c(\text{skin}-\text{air})}$ | convection heat transfer coefficient between the skin and the air layer | $W{\cdot}m^{-2}{\cdot}K^{-1}$ |
| $H_{mi}$ | diffusion mass transfer coefficient between inner node and outer node | $kg{\cdot}m^{-2}{\cdot}kPa^{-1}{\cdot}s^{-1}$ |
| $H_{mo}$ | mass transport coefficient between outer node and air void in the fabric | $kg{\cdot}m^{-2}{\cdot}kPa^{-1}{\cdot}s^{-1}$ |
| $h_{m(\text{skin}-\text{air})}$ | mass transfer coefficient between the skin and the air layer | $kg{\cdot}m^{-2}{\cdot}kPa^{-1}{\cdot}s^{-1}$ |
| $h_r$ | radiative heat transfer coefficient | $W{\cdot}m^{-2}{\cdot}K^{-1}$ |
| $I_T$ | total dry heat resistance of clothing ensemble | $m^2{\cdot}K{\cdot}W^{-1}$ |
| $I_{a-sk}$ | evaporative resistance of the trapped air layer over the skin | $m^2{\cdot}kPa{\cdot}W^{-1}$ |
| $k$ | thermal conductivity | $W{\cdot}m^{-1}{\cdot}K^{-1}$ |
| $M$ | metabolic rate production | $W{\cdot}m^{-2}$ |
| $\dot{m}_a$ | air mass flow rate through the fabric | $kg{\cdot}s^{-1}$ |
| $m_{as}$ | moisture accumulating on the skin | $kg{\cdot}m^{-2}$ |
| $m_{bl}$ | blood flow | $kg{\cdot}m^{-2}{\cdot}s^{-1}$ |
| $m_{rsw}$ | local sweat rate | $kg{\cdot}m^{-2}{\cdot}s^{-1}$ |
| $Q$ | heat loss | W |
| $P_a$ | air vapor pressure | kPa |
| $P$ | vapor pressure of water vawpor adsorbed in inner node | kPa |
| $P_\infty$ | water–vapor pressure in the environment | |
| $P_{\infty,t}$ | total air pressure in the environment | |
| $P^*$ | saturation pressure | kPa |
| $R$ | total regain in fabric | kg of adsorbed $H_2O{\cdot}kg^{-1}$ fiber |
| $R_v$ | water vapor gas constant | |
| $R_{ET}$ | evaporative resistance | $m^2{\cdot}kPa{\cdot}W^{-1}$ |
| $RH$ | relative humidity | % |
| $S_{cr}$ | heat storage of the core of the body | $W{\cdot}m^{-2}$ |
| $S_{sk}$ | heat storage of the skin of the body | $W{\cdot}m^{-2}$ |
| $T$ | temperature | (°C, K) |
| $t$ | time | s |
| $u_{ad}$ | internal energy of water in adsorbed state | $J{\cdot}kg^{-1}$ $H_2O$ |
| $u_f$ | total internal energy of fiber containing adsorbed $H_2O$ | $J{\cdot}kg^{-1}$ of dry fiber |
| $W$ | mechanical power accomplished | $W{\cdot}m^{-2}$ |
| $w$ | humidity ratio | kg of water·$kg^{-1}$ of air |
| $y$ | the instantaneous air spacing thickness | m |

*Greek symbols*

| | |
|---|---|
| $\alpha$ | air permeability |
| $\beta$ | ratio of skin node mass to total body mass |
| $\varepsilon$ | porosity |
| $\rho$ | mass density of fabric $kg{\cdot}m^{-3}$ |
| $\gamma$ | fraction of mass that is in the outer node |
| $\sigma$ | Stefan Boltzman constant, $= 5.669 \times 10^{-8}$ $W{\cdot}m^{-2}{\cdot}K^{-4}$ |
| $\tau$ | period of oscillation s |

*Subscripts*

| | |
|---|---|
| $a$ | conditions of air in the spacing layer between skin and fabric |
| $cr$ | core of the human body |
| $f$ | fabric |
| $i$ | inner node |
| $mb$ | mean body condition |
| $o$ | outer node |
| $L$ | latent |
| $res$ | respiration |
| $S$ | sensible |
| $sk$ | skin of the human body |
| void | local air inside the voids of the fabric |
| $\infty$ | environment ambient conditions |

garments during motion and the air penetration through the outer material. Lotens' clothing ventilation model, however, is not based on thermal principles, and has not taken into account any non-equilibrium heat and moisture adsorption processes that take place in the fabric layers [2].

Traditionally, models of heat and mass transfer through clothing layers focused on the simplified diffusion phenomena of heat and moisture transfer. These models assumed instantaneous equilibrium between the local relative humidity of the diffusing moisture and the regain of the fiber, and ignored the effect of ventilation on the heat and moisture exchange between the microclimate of the clothing and the ambient air. Farnworth developed a numerical model that took into account the condensation and adsorption in a multi-layered clothing system by developing linear relations to represent the fiber regain equilibrium [3]. Jones and Ogawa developed another model that used actual empirical relation obtained from experiments to calculate the fiber re-

gain equilibrium [4]. The latter model also took into account the sorption behaviour of fibers. The above-mentioned models focused on the diffusion process of heat and water vapor transport, and assumed instantaneous equilibrium between the local relative humidity of the penetrating air and the moisture content of the fiber. However, the hypothesis of local thermal equilibrium was shown to be invalid during periods of rapid transient heating or cooling in porous media as reported by Mincowycs et al. [5]. Their results for 1-$D$ porous layer show that in the presence of flow, local thermal equilibrium is not valid if the ratio of the Sparrow number to Peclet number is small. In the absence of local thermal equilibrium, the solid and the fluid should be treated as two different systems. Gibson conducted a two-dimensional numerical modelling and experimental testing of steady diffusion/convection processes in textiles [6–10]. The numerical model of Gibson included diffusion and convective transport of heat and moisture, as well as liquid water wicking through porous textile material. Gibson's model was based on Whitaker's theory [11] for mass and energy transport through porous media that assumes local thermodynamic equilibrium between the various phases that could exist in the porous textile material and ignored the possible existence of micro-scale pore-level heat and mass transfer coefficients. Under vigorous movement of a relatively thin porous textile material, the air will ventilate the fibers and the assumption of local thermodynamic equilibrium is invalid. Ghali et al. studied the effect of ventilation on heat and mass transport through fibrous material by developing a theoretical two-node absorption model, aided by experimental results on moisture regain of ventilated fabric, to predict the transfer coefficients of a cotton fibrous medium [12]. Their model was further developed and experimentally verified to predict temporal variations in temperature and moisture content of the air within the fiber in a multi-layer three-node model [13].

In realistic applications, ventilation of the clothing system during the human motion occurs by the periodic motion of air in and out of the air spacing, as the fabric moves outward or inward towards the skin. Ghali et al. reported original experimental data on sensible and latent heat transport initiated by sinusoidal motion of a fabric plane about a fixed mean air spacing thickness above a sweating isothermal hot plate placed in a controlled environment [14]. They developed a transient model that predicted the heat loss from the wet boundary and agreed fairly well with the experimentally measured values. Their transient model has not considered the coupling of the fabric model with the human body model that has variable skin humidity and temperature conditions based on the level of activity of the human [14]. The coupling of fabric models with human thermal models and human thermoregulatory response to heat and cold adds difficulty to the modeling of heat and mass transport from the body. Previously, Gagge et al. [15] developed a two-node model for describing the thermoregulatory system of the human body. In the model, they described the role of clothing in heat and moisture transport as the intrinsic insulation of the clothing and the intrinsic vapor resistance through the clothing, which are considered constant. This is true for steady state conditions when the body-clothing-environment system is isothermal. In order to describe the dynamic behavior, Jones et al. described a model of the transient response of clothing systems, which took into account the sorption behavior of fibers, but assumed local thermal equilibrium with the surrounding air [16]. They compared the prediction of heat loss by the model with experimental data from thermal manikin dry tests and found reasonable agreement. Recently, Li and Holocombe developed a mathematical model in which Gagge's two-node human thermoregulatory model was combined with a kinetic sorption model of fabrics to study the transient thermal response of a clothed human [17]. Their model, however, neglected the effect of ventilation between air passing through the fiber and the solid fiber. The periodic ventilation effect, according to Ghali et al. [14], causes a temperature change of about 2.5 °C in the enclosed air layer temperature during one period of oscillation of the fabric. For decades, the so-called pumping or bellows effect has been studied, and its importance on the heat and mass transfer of the human body has often been discussed [18–29]. The thermal manikin standing or movable has been used frequently to determine the insulation and evaporative resistance values of ensembles [27–30]. Static insulation databases of clothing insulation values, for a number of ensembles, are reported by McCullough et al. ASHRAE standard [18]. Hong presented data from a movable thermal manikin on the effect of walking on the clothing dry insulation values [19]. However, the database is limited to 24 ensembles and large deviations exist when regression analysis is used to predict the insulation value changes due to the walking effect. Havenith et al. quantified the effects of body movement, posture and wind through linear regression equations on the resultant measured clothing dry insulation, using the method of wrapping subjects by plastic foils [27]. The results, together with those from human studies, have yielded useful empirical information and data on the effect of activity on ensemble insulation. However, few investigations have dealt with the mechanisms behind the internal convection in the air layer adjacent to the body. Clothing heat and mass transfer mechanisms of a clothed walking human are not easily derived from current engineering literature since fluctuating airflow in a channel with a variable gap width is not a common engineering application. Berger and Sari developed a dynamic clothing model where they simulated the heat and mass transfers by renewal of the air confined under garment and coupled them to the heat and mass exchanges between the external side of the clothing and the outer environment including solar radiation flux exchanges [31]. The model used variable insulation values of Havenith et al. [27], variable inner convective coefficients and air velocity that were taken from experiments on heated manikin. However, the model

of Berger and Sari used zero-thickness garment with no calorific capacity and assumed exponential heating in the air layer and fixed skin temperature [31]. These assumptions neglected the ventilation in the fabric itself and considered the air void in the fabric at local thermal equilibrium with the fabric solid phase.

In this work, experiments are conducted to determine evaporative and dry film coefficients between skin and adjacent air layer during ventilation. A mathematical 1-D of the human body, the oscillating trapped air layer gap width, and the periodically-ventilated fabric will be developed and built from first principles of mass and energy balances to predict the effect of walking on exchanges of heat and mass and the reduction of the dynamic dry resistances of ensembles. The developed 1-D mathematical model uses Gagge's two-node human thermoregulatory model [15], combined with Ghali et al. fabric three-node model [13].

## 2. Experimental determination of the mass transfer coefficient "$h_{m(\mathbf{skin-air})}$" between the skin and the air layer

The film coefficients at the skin are needed for the model simulation. However, transport coefficients from the skin to the environment or clothing are reported in literature as a function of an effective wind velocity based on empirical work [21]. Most of the research is focused on estimating the heat transfer coefficient at the external exposed surface of clothing subject to elevated air velocities [32,33]. Such correlation would not be applicable for estimating the film coefficients in an enclosed air subject to an oscillatory flow. For this reason, experiments were conducted to measure the mass transfer coefficient at the skin to the air layer and then, using the Lewis relationship, to estimate the heat transfer coefficient as well from the skin to the air layer as well.

Untreated cotton was chosen as a representative of a most common worn fabric to test the behaviour when subject to periodic motion above the skin. The cotton was obtained from Test fabrics Inc. (Middlesex, NJ 08846), and is made of unmercerized cotton duck, style #466 of thickness of 1 mm. Fig. 1 shows front and top views of the experimental setup, which is composed of two square wooden frames, hinged to each other. Both frames have an inner open area of 0.508 m × 0.508 m and an outer area of 0.554 m × 0.554 m for the upper frame and an area of 0.585 m × 0.585 m for the lower one. The upper frame is connected to a rotating shaft. The shaft is connected to a gear motor. When the shaft rotates, the upper frame moves sinusoidally in a vertical path away and towards the lower frame in a stroke of 12.7 mm. The side view of the experimental set up shows the four-bar linkage mechanism by which the fabric is moved up and down. The hinges (piano hinges) were necessary to insure that the upper frame is moving in a horizontal plane without tilting. The cotton fabric was taped to the upper frame by an aluminum tape, and the exposed surface of

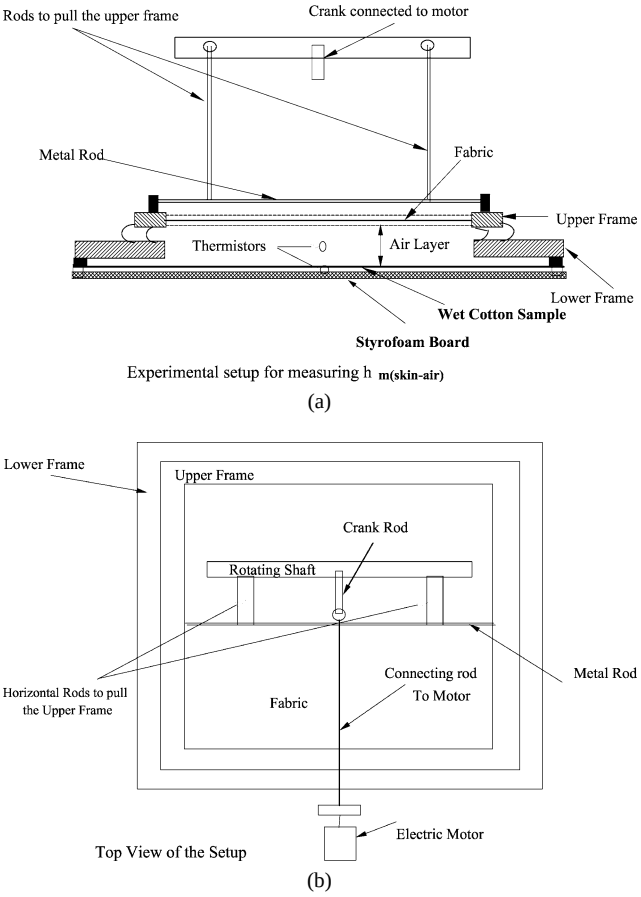


Fig. 1. The front (a) and top (b) views of the experimental setup.

both wooden frames was also covered by aluminum tape. To insure a planar movement of the fabric (no flattering) the fabric sample was placed between two metallic screens that were made of 12.7 mm open squares.

The movement of the fabric that is attached to the upper frame will cause air to move back and forth across the fabric. To reduce the possibility of air escaping through the hinges or through the lower frame, the hinges were covered with plastic wrapping and plastic foam was taped to the outer rim of the lower frame as shown in Fig. 1. A minimal layer of plastic wrapping was used to minimize possible horizontal movement of the air layer between the lower and upper frame. In the plane slightly above the fabric frame plane, an air circulation fan is placed to provide sufficient circulation of air (0.7 $\mathrm{m{\cdot}s^{-1}}$) for maintaining the constant chamber ambient conditions above the fabric. Before the start of the experiment, the whole frame was conditioned for 16 h inside an environmental chamber, not shown in the figures, at conditions of 25 °C and 50% *RH*. Then the frame was placed above a water saturated cotton sample. This wet cotton sample representing the skin was placed on top of an insulating Styrofoam board to create an adiabatic saturated boundary condition. The whole setup (fabric oscillating frame, wetted cotton sample and Styrofoam board shown in Fig. 1) was placed inside the environmental chamber whose

temperature conditions were set at 25 °C and 50% *RH*. The precision in the set conditions of the climatic chamber temperature was ±0.5 °C and chamber relative humidity was ±2%. The mean air spacing between the fabric and the adiabatic wet surface was 38.1 mm. The amplitude of oscillation was 6.35 mm. Experiments are conducted for gear motor frequencies are 27, 37 and 54 rpm.

At the beginning of the experiment, the saturated fabric sample (skin) was weighed and its weight loss of moisture was monitored every half an hour for a total of four hours. So every half hour the wet fabric sample was quickly removed and placed inside a plastic bag for weighing using a sensitive scale of accuracy ±0.01 g. The experiment started with oscillating the upper fabric and frame at the same frequency and amplitude conditions of the main experiment. Measuring of the temperature of the wetted cotton sample was monitored by a thermistor, while the temperature measurement of the air layer was measured by a radiation-shielded thermistor. One thermistor was placed on the lower surface of the wet cotton sample and above the Styrofoam board, while the other thermistor was placed in the enclosed air spacing between the oscillating fabric and the wet cotton surface. The accuracy of the temperature readings was ±0.1 °C.

Knowing the amount of water that evaporated from the fabric, the temperature of the wet cotton sample, the temperature of the air layer and the skin mass transfer coefficient can be estimated as follows:

$$m_s = h_{m(\text{skin}-\text{air})} A (P_{sk} - P_a) \tag{1a}$$

where $m_s$ is the measured mass flux ($\text{g}\cdot\text{s}^{-1}$), $P_a$ is the vapor pressure of the air (kPa), $P_{sk}$ is the vapor pressure at the skin (kPa) and $A$ is the area of the fabric ($\text{m}^2$). The vapor pressure at the skin is estimated from the equilibrium vapor pressure at the skin temperature, which remained at a uniform value of 21.0 ± 0.7 °C. The air layer vapor pressure is estimated from the temperature of the air layer and the wet bulb temperature of the air layer. The wet bulb temperature of the air layer is taken as that of the saturated skin temperature since the set up is similar to an adiabatic saturator for the enclosed air. The measured temperature of the wet skin sample did not change since the sample was wet during the time of the experiment. At 27 rpm, the measured evaporation rate starting from the second hour became steady at a value of 5 g every half an hour from which the mass transfer coefficient of $8 \times 10^{-5}$ $\text{kg}\cdot\text{s}^{-1}\cdot\text{m}^{-2}\cdot\text{kPa}^{-1}$ was determined. The mass transfer coefficients at the other two ventilation frequencies of 37 and 54 were $8.16 \times 10^{-5}$ and $9.216 \times 10^{-5}$ $\text{kg}\cdot\text{s}^{-1}\cdot\text{m}^{-2}\cdot\text{kPa}^{-1}$, respectively. A linear correlation is derived for $h_{m(\text{skin}-\text{air})}$ as a function of frequency for use in the numerical simulation parametric runs, and is given by

$$h_{m(\text{skin}-\text{air})} = (2.777 f + 6.635) \times 10^{-5} \tag{1b}$$

where $f$ is the frequency (Hz). The correlation parameter is 0.968. The dry convective heat transport coefficient from the skin to the lumped air layer $h_{c(\text{skin}-\text{air})}$ is then found from the Lewis relation for air–water vapor mixtures as $h_{c(\text{skin}-\text{air})} = h_{m(\text{skin}-\text{air})} h_{fg}/16.5$ [34].

Much less data is available on dynamic vapor resistance or mass transport coefficients than on convective dry insulation. The most comprehensive data on dynamic clothing dry insulation and water vapor resistances originated from Havenith et al. [27,28] using tracer gas instead of water vapor. Havenith et al. described the changes in clothing total, intrinsic and surface air layer insulation values [27] and vapor resistance values [28] due to the motion of the wearer and the wind for three ensembles. The situation of the current work is that of a very light, highly air permeable fabric with closed aperture garment. According to Lotens [2], the total insulation and vapor resistances in this case will be highly dependent on the air insulation that is described as a function of the effective wind velocity. Lotens reported evaporative resistance in 2-layer clothing at the skin to the clothing layer for various garments and apertures [2]. The data of Lotens are shown in Table 1 for closed aperture high air permeable cotton clothing at various walking speeds and winds [2]. The published experimental data on dynamic clothing insulation of surface air layer of Havenith et al. [27] are also given in Table 1 for a clothing ensemble of cotton/polyester workpants, polo shirt, sweater, socks and running shoes, and the present work range values of the dry convective transport coefficients from the skin to the internal air layer. The reported experimental data of Havenith et al. were based on measurements of dry heat loss where the subject skin was wrapped tightly with a thin, water–vapor impermeable, synthetic foil. Danielsson reported internal forced convection coefficients, as given in Table 1, for various parts of the body for loose fitting ensemble at walking speeds of 0.9, 1.4 and 1.9 $\text{m}\cdot\text{s}^{-1}$ [21]. The present work convective coefficients measurements were based on the evaporative heat loss and the moisture adsorption in the clothing only due to normal ventilation action of the fabric. The present experimental findings of convection coefficients are within 8% from the findings of Danielsson at the walking speed of 0.9 $\text{m}\cdot\text{s}^{-1}$ for the trunk and the arm parts of the body. The results still fall within a very sound range of real subjects experiments even though the reported data are for a different experimental setting and clothing ensembles.

## 3. Mathematical formulation of the system

In walking conditions, the air spacing between the fabric layer and the human skin changes with the walking frequency. This change will cause air penetration in and out of the clothing system depending on the fabric air permeability. The air passing through the fabric can considerably reduce the heat and moisture transfer resistance of the clothing system and its suitability for a given thermal environment. The purpose of clothing is to maintain a uniform body temperature under different temperature environments and to prevent

Table 1
Mean skin mass transfer coefficients as reported by Lotens [2], external surface air ($I_a$) insulation values, convective heat and mass transport coefficients reported by Havenith et al. [27,28], heat convection coefficient from skin to internal air film reported by Danielsson [21], and measured values of skin mass and heat transport coefficients in the present work

| Lotens' data [2] | | | Havenith et al. [27,28], ensemble A | | | | |
|---|---|---|---|---|---|---|---|
| Wind speed ($m\cdot s^{-1}$) | Walking speed ($m\cdot s^{-1}$) | $h_{m(skin-fabric)}$ ($kg\cdot s^{-1}\cdot m^{-2}\cdot kPa^{-1}$) | Walking speed ($m\cdot s^{-1}$) | Wind speed ($m\cdot s^{-1}$) | $I_a$ ($m^2\cdot k\cdot W^{-1}$) | $h_{c(skin-\infty)}$ ($W\cdot m^{-2}\cdot K$) | $h_{m(skin-\infty)}$ ($kg\cdot s^{-1}\cdot m^{-2}\cdot kPa^{-1}$) |
| 0.2 | 0 | $7.96\times10^{-5}$ | 0.3 | 0 | 0.093 | 10.093 | $6.943\times10^{-5}$ |
| | 0.694 | $10.69\times10^{-5}$ | | 0.7 | 0.061 | 16.39 | $11.0\times10^{-5}$ |
| | 1.388 | $12.79\times10^{-5}$ | | 4.0 | 0.032 | 31.25 | $21.9\times10^{-5}$ |
| 0.7 | 0 | $9.07\times10^{-5}$ | 0.9 | 0 | 0.097 | 10.31 | $7.09\times10^{-5}$ |
| | 0.694 | $12.68\times10^{-5}$ | | 0.7 | 0.067 | 14.925 | $10.09\times10^{-5}$ |
| | 1.388 | $13.24\times10^{-5}$ | | 4.0 | 0.026 | 38.26 | $26.3\times10^{-5}$ |

Measured heat transport coefficient from the skin to the air layer as reported by Danielsson [21]

| | | | |
|---|---|---|---|
| Walking speed ($m\cdot s^{-1}$) | 0.9 | 1.4 | 1.9 |
| $h_{c(skin-air)}$ ($W\cdot m^{-2}\cdot K^{-1}$): [Leg] | 13.7 | 17.4 | 19.0 |
| $h_{c(skin-air)}$ ($W\cdot m^{-2}\cdot K^{-1}$): [Trunk] | 10.2 | 13.0 | 15.1 |
| $h_{c(skin-air)}$ ($W\cdot m^{-2}\cdot K^{-1}$): [Arm] | 11.3 | 15.0 | 17.2 |

Present work data

| | | | |
|---|---|---|---|
| $f$ (rpm) | 27 | 37 | 54 |
| $h_{m(skin-air)}$ ($kg\cdot s^{-1}\cdot m^{-2}\cdot kPa^{-1}$) | $8.0\times10^{-5}$ | $8.16\times10^{-5}$ | $9.216\times10^{-5}$ |
| $h_{c(skin-air)}$ ($W\cdot m^{-2}\cdot K^{-1}$) | 11.6 | 11.9 | 13.265 |

the accumulation of sweat on the human skin by allowing the respired body water to flow to the outside environment when the activity level increases.

The human-clothing-environment system is schematically illustrated in Fig. 2(a). The human body is represented by a two-node model developed by Gagge et al. [15] with the core as the human inner node and the skin as the human outer node. The moving clothing system is represented by the three node-model of Ghali et al. [13,14]. An enclosed air layer separates the upper boundary (fabric) and the human skin. The upper boundary has a sinusoidal up and down motion that induces the air movement through the fabric. The size of the air spacing between the skin and the fabric is continuously varying in time depending on activity level and location, thus inducing variable airflow in and out of the fabric. The frequency of the oscillating motion of the fabric is assumed directly proportional to the activity level of the walking human. The air spacing layer beneath the fabric will be formulated as a lumped compressible layer with its density being a function of temperature and pressure.

The analysis of the airflow through the fabric is based on a single lumped fabric layer of the three-node adsorption model of the fibrous medium and an air void as shown in Fig. 2(b). The fabric outer node represents the exposed surface of the yarns, which is in direct contact with the penetrating air in the void space between the yarns. The fabric inner node represents the inner portion of the "solid" yarn, which is completely surrounded by the fabric outer node. The moisture uptake in the fabric occurs first by the convection effect at the yarn surface (outer node), followed by sorption/diffusion to the yarn interior (inner node). Wicking is assumed negligible in the fabric model

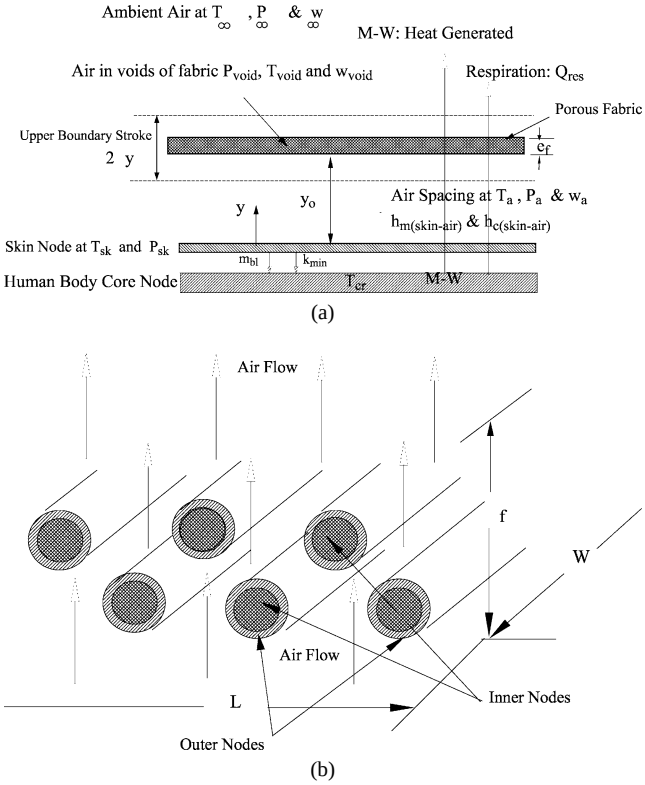


Fig. 2. Schematic of the human-clothing-environment system (a) and of the fabric model (b).

so that only solid and gas phases are present in the fabric. The clothing-fabric area is $A$ and the fabric thickness is $e_f$. The airflow is assumed normal to the fabric plane, which

represents the case of a fully clothed human with tight openings at the neck, wrists and legs.

### 3.1. Fabric and air layer model

#### 3.1.1. Modeling of the air mass flow rate through the fabric

The fabric sinusoidal motion can be represented by the following equation:

$$y = y_0 + \Delta y \sin(2\pi f t) \tag{2}$$

where $y$ is the sir spacing thickness, $f$ is the frequency of oscillation, $y_0$ is the mean air spacing thickness (38.1 mm) and $\Delta y$ is the oscillation amplitude (6.35 mm). Conducting a mass balance for the skin-fabric air layer leads to

$$-\dot{m}_a = \frac{\partial}{\partial t}(\rho_a y) \tag{3a}$$

where $\dot{m}_a$ is the air mass flow rate and $\rho_a$ is density of air. The negative sign indicates that the airflow direction is opposite to the direction of fabric motion. Eq. (3a) can be expanded to the following:

$$-\dot{m}_a = y\frac{\partial}{\partial t}(\rho_a) + \rho_a \frac{\partial}{\partial t}(y) \tag{3b}$$

Note that the air layer above the fabric is moving and represents a boundary condition, with constant temperature and humidity. As the fabric moves down, the airspace between the skin and the fabric moves out through the fabric and is swept away by the moving air stream. When the direction of the fabric reverses, the opposite process occurs. That is, the void created as the fabric rises is filled with air from the moving air stream that passes through the fabric.

When there is pressure difference between the fabric surfaces, there will be a mass flowing through the fabric. The amount of the air depends on the permeability of the fabric material. The permeability $\alpha$ is affected by the type of yarn, tightness of twist in yarns, yarn count and fabric structure. In this study, the permeability of the fabric is considered constant at the standard experimentally measured value under the pressure difference of 0.1245 kPa. To get the airflow passing through the fabric at other pressure differentials, the air permeability is assumed to be constant and the amount of airflow is proportional to the pressure differentials. The airflow rate is then represented by

$$\dot{m}_a = \frac{\alpha \rho_a}{\Delta P_m}(P_a - P_\infty) \tag{4}$$

where $\alpha$ is the fabric air permeability ($\alpha = 4.99\ \mathrm{cm^3 \cdot cm^{-2} \cdot s^{-1}}$) and $\Delta P_m = 0.1245$ kPa from standard tests on fabrics' air permeability [ASTM D737-75], $P_a$ is the air pressure of the air layer between the skin and the fabric and $P_\infty$ is the outside environment water vapor pressure. Substituting the ideal gas relation, $\rho_a = P_a/R_a T_a$, into Eq. (3b) gives the mass balance in the air spacing in terms of the air pressure as

$$-\frac{\alpha P_a}{R_a T_a \Delta P_m}(P_a - P_\infty) = \frac{y}{R_a T_a}\frac{\partial P_a}{\partial t} + \frac{P_a}{R_a T_a}\frac{\partial y}{\partial t} + \frac{y P_a}{R_a}\frac{\partial (1/T_a)}{\partial t} \tag{5}$$

from which the pressure $P_a$ can be determined as a function of time. Substituting $P_a$ into Eq. (4) gives the instantaneous air mass flow rate, which will be used in the fabric model.

#### 3.1.2. Modelling of the air-spacing layer

The air trapped between the skin and the fabric is renewed by the pumping action of the fabric boundary through the air voids of the fabric. The renewal is associated with variations of the dry and humid coefficients at the skin and fabric levels. During the upward motion of the fabric, the airflow into the air spacing layer comes from the air void node of the fabric and will have the same humidity ratio as the air in the void space of the fabric. The water vapor mass balance for the air spacing layer while the fabric is moving up is given by

$$\frac{\partial(\rho_a y w_a)}{\partial t} = h_{m(\mathrm{skin-air})}[P_{sk} - P_a] - \dot{m}_a w_{\mathrm{void}} + D\frac{\rho_a(w_{\mathrm{void}} - w_a)}{e_f/2} \tag{6a}$$

During the downward motion of the fabric, the airflow through the fabric out of the air spacing will carry the same humidity ratio of the air spacing. Then the water vapor mass balance for the air spacing layer during the downward motion is given by

$$\frac{\partial(\rho_a y w_a)}{\partial t} = h_{m(\mathrm{skin-air})}[P_{sk} - P_a] - \dot{m}_a w_a + D\frac{\rho_a(w_{\mathrm{void}} - w_a)}{e_f/2} \tag{6b}$$

where $h_{m(\mathrm{skin-air})}$ is the mass transfer coefficient between the skin and the air layer, $P_a$ is the water vapor pressure in the air layer, $w_a$ is the humidity ratio of the air layer, $P_{sk}$ is the vapor pressure at the skin solid boundary, $w_{\mathrm{void}}$ is the humidity ratio of the air void and $D$ is the diffusion coefficient of water vapor into air. The first term in Eqs. (6a) and (6b) represent the mass transfer from the skin to the trapped air layer, the second term is the convective mass flow coming through the fabric voids and the last term is the water vapor diffusion term from the air layer to the air in the fabric void due to difference in water vapor concentration.

The energy balance for the air-vapor mixture in the air spacing layer will be performed taking into account the motion direction of the fabric and its effect on the properties of the air mass that enters the domain during upward motion and that leaves the domain during the downward motion. An energy balance of the air spacing of the fabric expresses the rate of change of the energy air-vapor mixture of air-layer in terms of the external work done by the environment on the air layer, the evaporative heat transfer from the moist skin, the dry convective heat transfer from the skin, the convection of heat to the air layer associated with $\dot{m}_a$ coming through

the upper boundary and the heat diffusion from void air to confined air layer due to gradients in temperature and water–vapor concentrations. The energy balance during upward motion is given by

$$\begin{aligned}&\frac{\partial}{\partial t}\left[\rho_a y(C_v T_a + w_a h_{fg})\right] + P_{\infty,t}\frac{\partial y}{\partial t}\\&\quad = h_{m(\text{skin}-\text{air})}h_{fg}[P_{sk} - P_a] + h_{c(\text{skin}-\text{air})}[T_{sk} - T_a]\\&\qquad - \dot{m}_a[C_p T_{\text{void}} + w_{\text{void}}h_{fg}] + Dh_{fg}\frac{\rho_a(w_{\text{void}} - w_a)}{e_f/2}\\&\qquad + k_a\frac{(T_{\text{void}} - T_a)}{e_f/2}\end{aligned} \tag{7a}$$

During the downward motion of the fabric, the energy balance in the air spacing layer becomes

$$\begin{aligned}&\frac{\partial}{\partial t}\left[\rho_a y(C_v T_a + w_a h_{fg})\right] + P_{\infty,t}\frac{\partial y}{\partial t}\\&\quad = h_{m(\text{skin}-\text{air})}h_{fg}[P_{sk} - P_a] + h_{c(\text{skin}-\text{air})}[T_{sk} - T_a]\\&\qquad - \dot{m}_a[C_p T_a + w_a h_{fg}] + Dh_{fg}\frac{\rho_a(w_{\text{void}} - w_a)}{e_f/2}\\&\qquad + k_a\frac{(T_{\text{void}} - T_a)}{e_f/2}\end{aligned} \tag{7b}$$

where $k_a$ is the thermal conductivity of air. Since the fabric void thickness is very small, conduction of heat from the fabric void air to the trapped air layer is represented by the law of wall as shown in the last two terms of Eqs. (7a) and (7b).

### 3.1.3. Modeling of the fabric

In the fabric, the three-node adsorption model of Ghali et al. will be used to describe the heat and moisture transport through the fabric due to air ventilating motion [13]. The effective heat and mass transfer coefficients $H_{co}$ and $H_{mo}$ for the outer node of the fabric, and the heat and mass diffusion coefficients $H_{ci}$ and $H_{mi}$ for the inner nodes of the fabric, are used in the model in normalized form as follows [13]:

$$\begin{aligned}H'_{mo} &= H_{mo}\frac{A_o}{A_f}, \qquad H'_{co} = H_{co}\frac{A_o}{A_f}\\H'_{mi} &= H_{mi}\frac{A_i}{A_f}, \qquad H'_{ci} = H_{ci}\frac{A_i}{A_f}\end{aligned} \tag{8}$$

where $A_f$ is the overall fabric surface area, $A_o$ is the outer-node exposed surface area to air flow and $A_i$ is the inner node area in contact with the outer node. The outer node convection coefficients are function of the normal airflow rate across the fabric.

The water vapor mass balance in the air void node is given in Eqs. (9a) and (9b) during the upward motion and downward motion of the fabric, respectively as:

$$\begin{aligned}&\frac{\partial}{\partial t}(\rho_a e_f w_{\text{void}}\varepsilon_f)\\&\quad = -\dot{m}_a[w_\infty - w_{\text{void}}] + H'_{mo}[P_o - P_{\text{void}}]\\&\qquad + D\frac{\rho_a(w_a - w_{\text{void}})}{e_f/2} + D\frac{\rho_a(w_\infty - w_{\text{void}})}{e_f/2}\end{aligned} \tag{9a}$$

$$\begin{aligned}&\frac{\partial}{\partial t}(\rho_a e_f w_{\text{void}}\varepsilon_f)\\&\quad = \dot{m}_a[w_a - w_{\text{void}}] + H'_{mo}[P_o - P_{\text{void}}]\\&\qquad + D\frac{\rho_a(w_a - w_{\text{void}})}{e_f/2} + D\frac{\rho_a(w_\infty - w_{\text{void}})}{e_f/2}\end{aligned} \tag{9b}$$

where $\varepsilon_f$ is the fiber porosity and $e_f$ is the fabric thickness. The outer fiber node and the inner fiber node mass balances are given in Eqs. (10) and (11), respectively:

$$\frac{\mathrm{d}R_o}{\mathrm{d}t} = \frac{1}{\rho\gamma e_f}\left[H'_{mo}(P_{\text{void}} - P_o) + H'_{mi}(P_i - P_o)\right] \tag{10}$$

$$\frac{\mathrm{d}R_i}{\mathrm{d}t} = \frac{H'_{mi}}{\rho(1-\gamma)e_f}[P_o - P_i] \tag{11}$$

where $R_o$ is the regain of the outer node and $R_i$ is the regain of the inner node. The parameter $\gamma$ is the fraction of mass that is in the outer node and it depends on the fabric type and the fabric porosity and is taken as 0.6 to be consistent with the empirical transport coefficients [12]. The total regain $R$ in the fiber is given by

$$R = \gamma R_o + (1-\gamma)R_i \tag{12}$$

An energy balance for the air-vapor mixture in the air void node is given in Eqs. (13a) and (13b) during the upward motion and downward motion of the fabric, respectively as:

$$\begin{aligned}&\varepsilon_f\frac{\partial}{\partial t}\left[\rho_a e_f(C_v T_{\text{void}} + h_{fg}w_{\text{void}})\right]\\&\quad = -\dot{m}_a[C_p T_\infty + w_\infty h_{fg}] + \dot{m}_a[C_p T_{\text{void}} + w_{\text{void}}h_{fg}]\\&\qquad + H'_{co}[T_o - T_{\text{void}}] + k_a\frac{T_a - T_{\text{void}}}{e_f/2} + k_a\frac{T_\infty - T_{\text{void}}}{e_f/2}\\&\qquad + Dh_{fg}\frac{\rho_a(w_a - w_{\text{void}})}{e_f/2} + Dh_{fg}\frac{\rho_a(w_\infty - w_{\text{void}})}{e_f/2}\end{aligned} \tag{13a}$$

$$\begin{aligned}&\varepsilon_f\frac{\partial}{\partial t}\left[\rho_a e_f(C_v T_{\text{void}} + h_{fg}w_{\text{void}})\right]\\&\quad = \dot{m}_a[C_p T_a + w_a h_{fg}] - \dot{m}_a[C_p T_{\text{void}} + w_{\text{void}}h_{fg}]\\&\qquad + H'_{co}[T_o - T_{\text{void}}] + k_a\frac{T_a - T_{\text{void}}}{e_f/2} + k_a\frac{T_\infty - T_{\text{void}}}{e_f/2}\\&\qquad + Dh_{fg}\frac{\rho_a(w_a - w_{\text{void}})}{e_f/2} + Dh_{fg}\frac{\rho_a(w_\infty - w_{\text{void}})}{e_f/2}\end{aligned} \tag{13b}$$

The terms that appear in the energy balance includes energy associated with $\dot{m}_a$, convective energy transport to the fabric outer node by conduction and moisture adsorption and conduction and mass diffusion terms to both the air layer and environment. The energy balance on the outer nodes gives

$$\begin{aligned}\rho_f(1-\gamma)\left[C_{pf}\frac{\mathrm{d}T_o}{\mathrm{d}t} - h_{ad}\frac{\mathrm{d}R_o}{\mathrm{d}t}\right] &= \frac{H'_{co}}{e_f}[T_{\text{void}} - T_o]\\&- \frac{H'_{ci}}{e_f}[T_o - T_i] + \frac{h_r}{2e_f}(T_{sk} - T_o) + \frac{h_r}{2e_f}(T_\infty - T_o)\end{aligned} \tag{14}$$

where $h_{ad}$ is the enthalpy of the water adsorption state and $h_r$ is the radiative heat transfer coefficient. The density of the

adsorbed phase of water is similar to that of liquid water. The high density results in the enthalpy and internal energy of the adsorbed phases being very nearly the same. Therefore, the internal energy, $u_{ad}$, can be replaced with the enthalpy of the adsorbed water. Since liquid water represents the state of zero enthalpy, then for consistency, the enthalpy of the adsorbed state is the difference $(h_{fg} - h_{ad})$. Data on $h_{ad}$, as a function of relative humidity, is obtained from the work of Morton and Hearle [35]. Also the fabric is exchanging radiation heat with the plate and the chamber. The energy balance on the inner node gives

$$\rho_f \gamma \left[ C_{pf} \frac{\mathrm{d}T_i}{\mathrm{d}t} - h_{ad} \frac{\mathrm{d}R_i}{\mathrm{d}t} \right] = \frac{H'_{ci}}{e_f} [T_o - T_i] \tag{15}$$

The set of the above-coupled differential equations (6)–(15) describes the time-dependent convective mass and heat transfer from the skin-adjacent air layer through the fabric induced by the sinusoidal motion of the fabric. The diffusion and transport coefficients, namely $H'_{ci}$, $H'_{mi}$, $H'_{co}$ and $H'_{mo}$ appearing in the equation are obtained from the reported empirical results of Ghali et al. [13].

### 3.2. Gagge's human model description

The heat balance equation between body and surroundings can be expressed as:

$$S = M - W - \left[ A_d h_{c(\mathrm{skin-air})} (T_{sk} - T_a) + A_d h_r (T_{sk} - T_o) + A_d h_{m(\mathrm{skin-air})} h_{fg} (P_{sk} - P_a) \right] - Q_{res} \tag{16}$$

where $S$ is the rate of internal energy storage, $M$ is the metabolic heat generation rate during exercise and shivering rate, $W$ is the physical work done by the body and $Q_{res}$ is the total rate of heat loss by respiration. The terms between parentheses represent the convective heat, radiative heat and evaporative heat losses from the skin. The skin and the clothing are coupled by the air layer. The human body is represented by Gagge's two-node model, where two energy balance equations are written for the core node and the skin node. There are several ways to write these equations. Jones and Ogawa wrote these equations in the following form [4]:

$$S_{sk} = A_d (Q_{cr-sk} - Q_{sk}) + S_{cr-sk} \tag{17a}$$

$$S_{cr} = A_d (M - W - Q_{cr-sk} - Q_{res}) - S_{cr-sk} \tag{17b}$$

where

$$S_{cr-sk} = (K_{\min} + c_{bl} m_{bl})(T_{cr} - T_{sk}) \tag{17c}$$

$$S = S_{cr} + S_{sk} \tag{17d}$$

where $m_{bl}$ is the blood flow rate between skin and core and $K_{\min}$ is the thermal conductance between core and skin. The model is based on a standard man, with body surface area $(A_d)$ equivalent to the DuBois area (1.8 $\mathrm{m}^2$), mass (70.0 kg) and height (1.77 m).

The rate of energy storage is written in terms of the time rate of change of the temperature in each node:

$$S_{sk} = \frac{C_{sk}}{A_d} \frac{\mathrm{d}T_{sk}}{\mathrm{d}t} \tag{18a}$$

$$S_{cr} = \frac{C_{cr}}{A_d} \frac{\mathrm{d}T_{cr}}{\mathrm{d}t} \tag{18b}$$

$$\frac{\mathrm{d}T_{mb}}{\mathrm{d}t} = \beta \frac{\mathrm{d}T_{sk}}{\mathrm{d}t} + (1 - \beta) \frac{\mathrm{d}T_{cr}}{\mathrm{d}t} \tag{19}$$

where $C_{sk}$ and $C_{cr}$ are the heat capacity of the skin and core nodes, respectively. $T_{mb}$ is the mean body temperature and $\beta$ is the fractional skin node mass to the total body mass and depends on the blood flow rate between core and skin [4]. The blood flow rate between core and skin is controlled by the cold skin signal and the warm skin signals which allow the mass of each node to vary as well, resulting in a shift of internal rate of energy storage from one node to the other. All of the thermal functions in Gagge's model are controlled directly by the temperature signals except the skin mass fraction. The temperature signals are defined either as worm or cold depending on whether the core and skin temperatures are higher or lower than their thermoneutral values, i.e., 33.7 and 36.8 °C. Since the expressions of these thermal functions are explicitly described in the ASHRAE Handbook of Fundamentals, they will not be repeated here [34].

### 3.3. The skin surface

The instantaneous sensible heat exchange from the skin to the air layer is expressed in terms of the convection heat loss at the skin surface and the radiation exchange between the skin and the fabric. The skin temperature is an input boundary condition obtained from the thermoregulatory model of the human body model, while the convective coefficient is evaluated empirically from experimental measurements.

For the latent heat transfer, the boundary condition is more complex. If liquid is present on the skin surface then the skin boundary condition is the saturation pressure at the skin temperature $P_{sk} = P^*(T_{sk})$. Just because sweating occurs does not imply that there will be liquid on the skin surface. The vapor pressure at the skin surface is then determined by a balance between the diffusion of vapor through the skin, the sweat secreted and the transport of moisture away from the skin as reported by Jones et al. [36].

$$P_{sk} = \frac{[P^*(T_{sk})(I_{a-sk}) + P_a I_{sk} + m_{rsw} h_{fg} I_{sk}]}{(I_{sk} + I_{a-sk})} \tag{20}$$

where $I_{sk}$ is the evaporative resistance of the skin which is approximately 0.33 $\mathrm{m}^2 \cdot \mathrm{kPa} \cdot \mathrm{W}^{-1}$ for a well hydrated person, $I_{a-sk}$ is the evaporative resistance of the trapped air layer in $\mathrm{m}^2 \cdot \mathrm{kPa} \cdot \mathrm{W}^{-1}$ obtained from $h_{m(\mathrm{air-skin})}$ and $m_{rsw}$ is the local sweat rate ($\mathrm{kg} \cdot \mathrm{m}^{-2} \cdot \mathrm{s}^{-1}$) [37]. The value of the skin vapor pressure is subject to the constraint that the vapor pressure calculated in Eq. (20) cannot exceed the saturation pressure, $P_{sk} \leqslant P^*(T_{sk})$. Eq. (20) applies even if the sweat rate is zero. Jones [36] included the accumulation of moisture on the skin and the evaporation of that moisture in the boundary condition through a mass balance at the skin surface subject

to the constraint that the accumulated moisture is less than 0.035 kg·m$^{-2}$, based on the maximum sweat layer that can be sustained over the body, which is about 35 μm [38].

## 4. Numerical method

The metabolic rate of the body taken a walking person on a level surface is 115 and 150 W·m$^{-2}$ corresponding to walking speeds of 0.9 and 1.34 m·s$^{-1}$, respectively. The mean air spacing and amplitude of oscillation is assumed the same as that of the experiment. The numerical integration of Eqs. (16)–(19) starts from energy balances of the human core node where respiratory heat losses, and regulatory signal responses are calculated, and the skin surface vapor pressure and temperature are found from the skin heat balances and interaction with the core node and the air layer. In the runs the skin boundary conditions are regulated by the human metabolic rate and thermoregulatory responses model. The air layer is coupled to the three-node model of the fabric where the coupled eight mass and heat transport Eqs. (6), (7) and (9)–(15) of the outer and inner nodes of the fabric and the air void are integrated numerically using first-order Euler–Forward scheme with a time step size of 0.005 s, over a total integration period of 3600 s. The periods of oscillation in this work ranged from 0.8 to 3 s. The presented model is a lumped model for each of the spacing air layer and the fabric layer which allows simplicity in updating, in time, the dependent variables of temperature and humidity ratio at each node. The vapor pressure of the flowing air in the air spacing layer or in the fabric voids is related to the air relative humidity, "*RH*", and temperature, and is calculated using the psychrometric formulas of Hyland and Wexler [39] to predict the saturation water–vapor pressure and hence the vapor pressure at the specified relative humidity. The regain of the cotton material has a definite relation to the relative humidity of the water vapor through a property curve of regain versus relative humidity [35]. The graphical relation of $R$ as a function of relative humidity, *RH*, has been interpolated with third order polynomials for 10 relative humidity intervals from zero to 100%. The interpolation functions are used in the simulation to calculate the inner and outer nodes' relative humidities corresponding to the values obtained of inner and outer regains, respectively. At every time step, the air mass flow rate is updated and the total regain, and temperatures of all the nodes are evaluated. When the solution converges to a steady periodic solution, the cycle time-averaged sensible and latent heat loss from the skin are calculated using the experimentally evaluated heat and mass transfer coefficients $h_{c(\text{skin}-\text{air})}$ and $h_{m(\text{skin}-\text{air})}$ in the air spacing layer as:

$$\overline{Q}_S = A_d\left[h_{c(\text{skin}-\text{air})}\left\{\frac{1}{\tau}\int_t^{t+\tau}(T_{sk}-T_a)\,\mathrm{d}t\right\} + h_r\frac{1}{\tau}\int_t^{t+\tau}(T_{sk}-T_o)\,\mathrm{d}t\right] \tag{21a}$$

$$\overline{Q}_L = A\left[h_{fg}h_{m(\text{skin}-\text{air})}\left\{\frac{1}{\tau}\int_t^{t+\tau}(P_{sk}-P_a)\,\mathrm{d}t\right\}\right] \tag{21b}$$

and the average overall dry resistance of clothing, $I_T$ (clo), is determined by Jones and McCullough as [40]

$$I_T = \frac{A_d(T_{sk}-T_\infty)C}{\overline{Q}_S} \tag{22a}$$

where $C$ is the unit conversion constant = 6.45 clo·W·m$^{-2}$·°C, and the clo value is a standard unit for comparing clothing insulation. The total evaporative resistance, $R_{ET}$, provided by the fabric and the air film is given by [40]

$$R_{ET} = \frac{A_d(P_{sk}-P_\infty)}{\overline{Q}_L} \tag{22b}$$

Experimental data are available on dry heat resistance of many clothing ensembles, while evaporative heat resistance model calculations still remain untested with lack of experimental data in literature.

## 5. Results and discussion

The simulations are performed at three different metabolic rates of 115 and 150 W·m$^{-2}$. At each metabolic rate, different ventilation frequencies are used for consistency and sensitivity analysis. The initial conditions start from ambient conditions of 25 °C and 50% *RH*. Results of the transient thermal responses of temperature and moisture content of the human skin, air layer and the porous fabric, and sensible and latent heat loss from the skin are presented at different ventilation frequencies. This is followed by model validation by comparisons with published data.

Fig. 3(a) presents the predicted human skin temperature and Fig. 3(b) presents the air spacing layer temperature as a function of time at the metabolic rate of 115 W·m$^{-2}$ for the ventilation frequencies of 25, 45 and 60 rpm. The skin temperature and the air layer temperature decrease as the ventilation frequency increases. The ventilation frequency of a walking human at $M = 115$ W·m$^{-2}$ with a speed of 0.89 m·s$^{-1}$ will normally be about 45–60 rpm. This can be estimated based on the number of steps the walking human makes in one second. However, the same metabolic rate may be produced at different ventilation frequencies depending on the human weight, the subcutaneous fat layer, and the effort made while walking. The increase of the ventilation frequency will increase the transport of moisture and heat to the fabric. Fig. 4 presents the predicted total moisture regain of the fabric as function of time at $M = 115$ W·m$^{-2}$ for the ventilation frequencies of 25, 45 and 60 rpm. The regain increases sharply in the initial period of the start of activity, and then increases at a slower mean rate in an oscillating

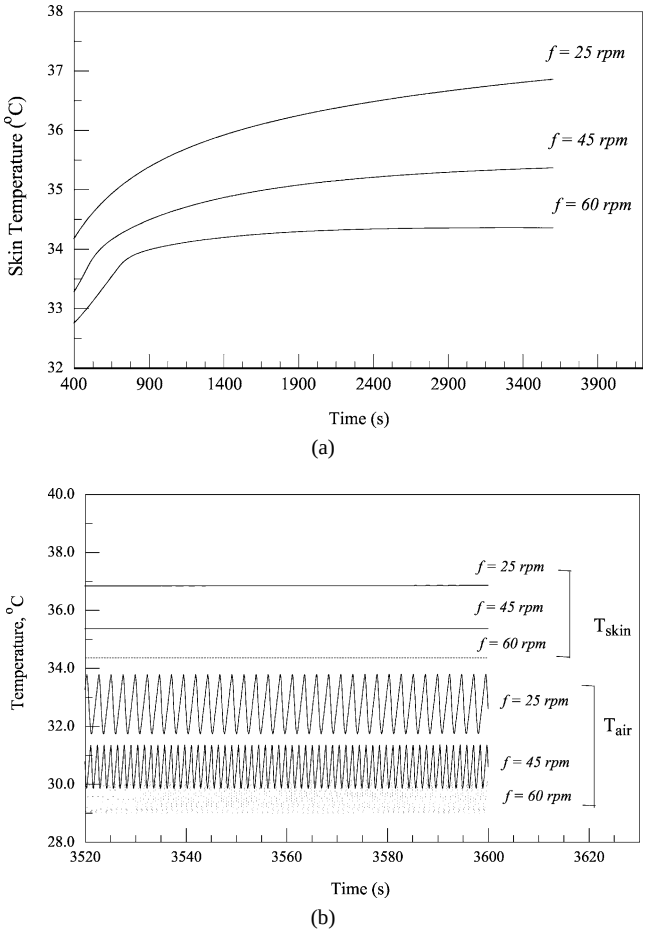


Fig. 3. (a) The predicted human skin temperature as a function of time at $M = 115$ W·m$^{-2}$ for the ventilation frequencies of 25, 45 and 60 rpm. (b) The predicted human skin temperature and the air layer temperature as a function of time at the metabolic rate of 115 W·m$^{-2}$ for the ventilation frequencies of 25, 45 and 60 rpm.

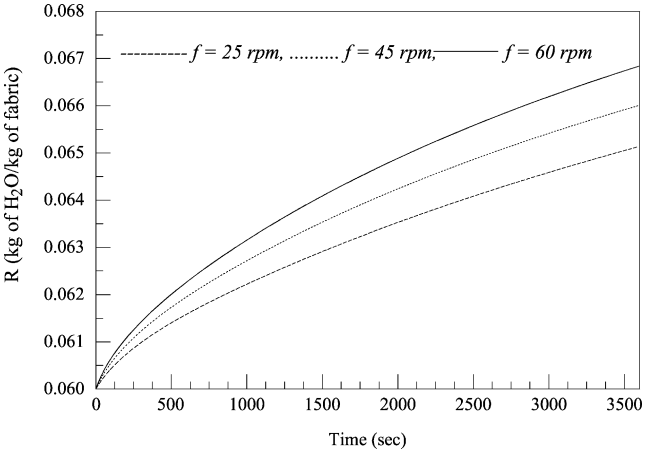


Fig. 4. The predicted total moisture regain of the fabric as function of time at $M = 115$ W·m$^{-2}$ for the ventilation frequencies of 25, 45 and 60 rpm.

pattern. When ventilation frequency is increased, the fabric regain increases as more moisture gets carried away from the human body surface. The temperature variation in time

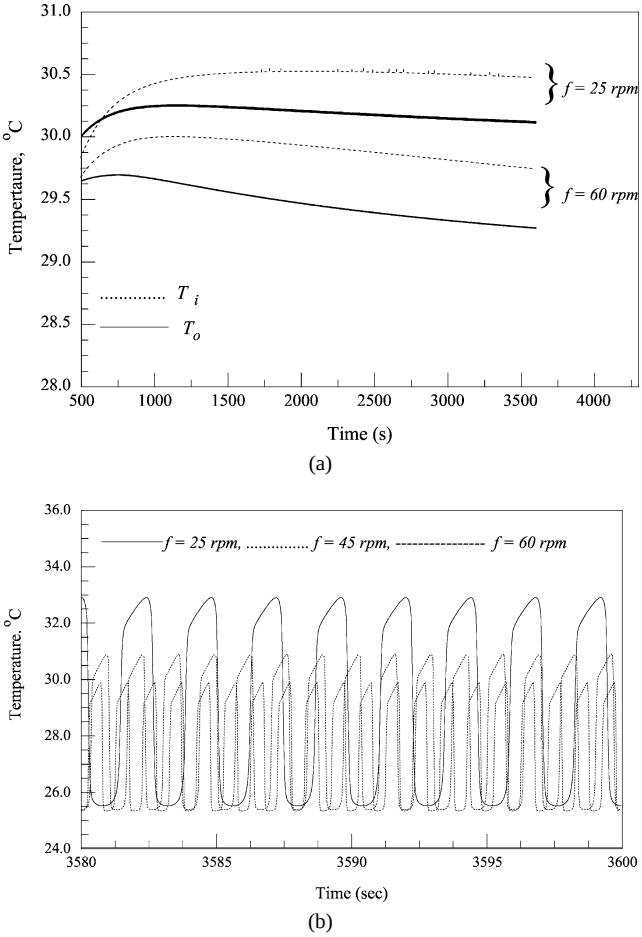


Fig. 5. (a) The temperature variation in time of the fabric inner and outer nodes at $M = 115$ W·m$^{-2}$ at different frequencies, with the steady periodic solution amplified. (b) The temperature variation in time of the fabric air void node at $M = 115$ W·m$^{-2}$ at different frequencies.

of the fabric inner and outer nodes is shown in Fig. 5(a) at $M = 115$ W·m$^{-2}$ at different frequencies, with the steady periodic solution amplified, while Fig. 5(b) shows the air–void node temperature variation. The outer node temperature attains a sinusoidal pattern similar to the forcing motion, but the inner node is less sensitive to external variations since heat and mass transfer diffusion to the inner node is a slower process than the ventilation of the outer node. The air–void node temperature has the largest temperature change during the oscillation cycle, since it is the mediating node between the environment and the air layer adjacent to the human skin. Fig. 6(a) shows a plot of the humidity ratio of the air layer as a function of time, and Fig. 6(b) shows the humidity ratio at the skin where the steady periodic solution is reached for various ventilation frequencies. As the frequency increases, less moisture is present at the surface of the skin.

Figs. 7(a) and 7(b) show the predicted steady periodic sensible and latent heat losses from the skin at the $M = 115$ W·m$^{-2}$ at $f = 25$, 45 and 60 rpm. The sensible heat loss increases with increased ventilation frequency. Since dry environment conditions prevail, the heat transfer

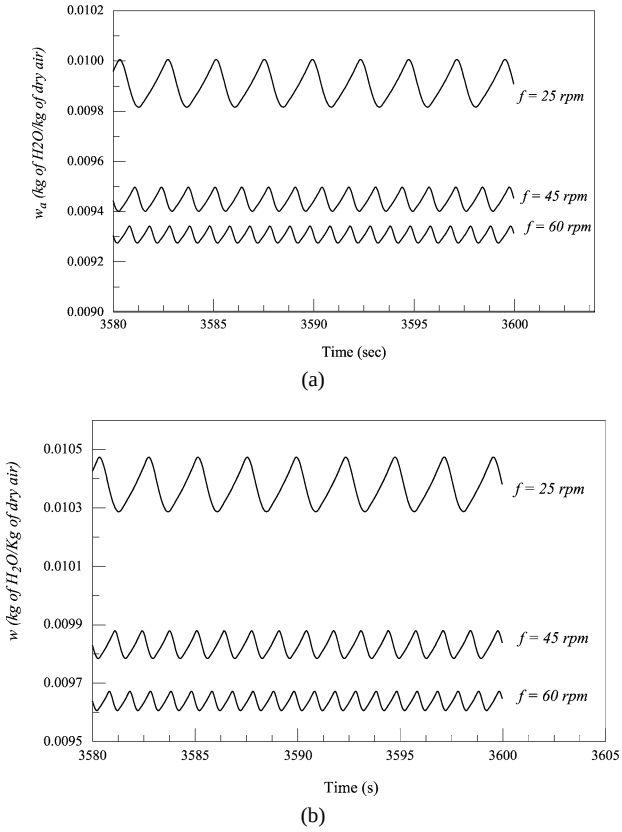


Fig. 6. (a) The humidity ratio of the air layer as a function of time for the various ventilation frequencies at $M = 115$ W·m$^{-2}$. (b) The humidity ratio of the skin as a function of time, for various ventilation frequencies at $M = 115$ W·m$^{-2}$.

is dominated by dry convection and radiation more than moisture evaporation. Increasing the ventilation frequency at fixed metabolic rate causes the skin temperature to drop and hence the skin water–vapor pressure drops resulting in dryer skin. This explains the drop in the latent heat loss from the skin with increased ventilation frequency. When the metabolic rate is increased, higher latent and sensible heat losses are expected from the body. As the solution reaches the steady periodic state, the time-averaged sensible heat loss from the skin at $f = 25$, 45 and 60 rpm are 147, 168 and 174 W, respectively. The time-averaged latent heat loss from the skin at $f = 25$, 45 and 60 rpm are 24.1, 25.8 and 28.2 W, respectively. Figs. 8(a) and 8(b) present the sensible and latent heat losses at $M = 150$ W·m$^{-2}$ for the frequencies $f = 50$ and 75 rpm. An increase of metabolic rate from 115 W·m$^{-2}$ at 25 rpm to 150 W·m$^{-2}$ at 35 rpm resulted in an increase of the latent heat loss by 4.7% due to sweating and an increase of sensible heat loss by 21%.

Fig. 9 shows the predicted overall (a) dry insulation and (b) evaporative resistance values of the clothing system at the $M = 115$ W·m$^{-2}$ at $f = 25$, 45 and 60 rpm. Fig. 10 shows the predicted overall (a) dry insulation and (b) evaporative resistance values of the clothing system at the $M = 150$ W·m$^{-2}$ at $f = 50$ and 75 rpm. In the present model, the time-averaged dry insulation values from Eq. (22a) averaged

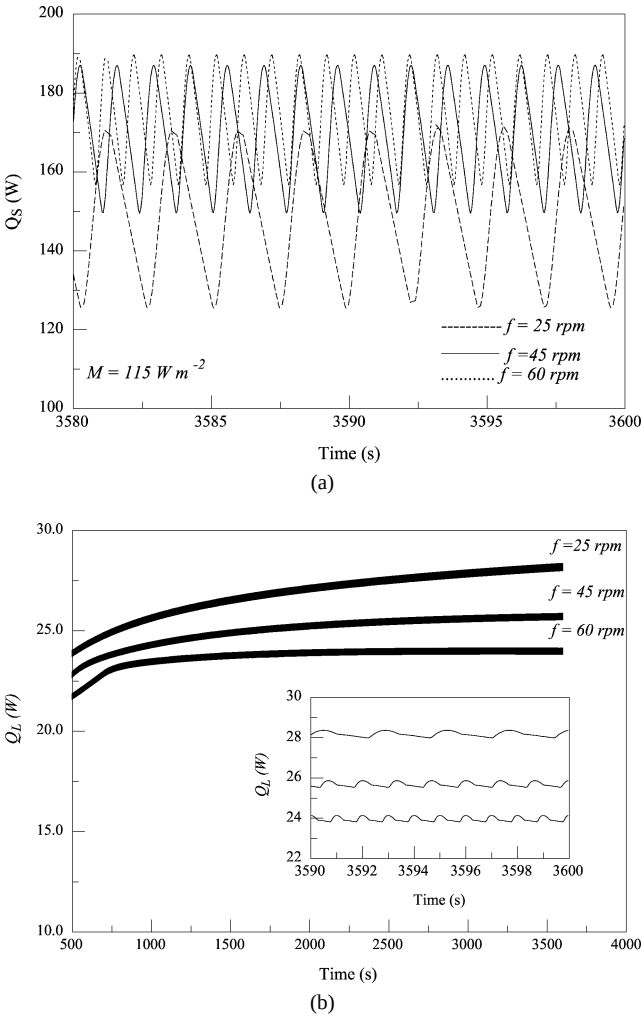


Fig. 7. (a) The predicted steady periodic sensible heat loss as a function of time from the skin for $M = 115$ W·m$^{-2}$ at $f = 25$, 45 and 60 rpm. (b) The predicted latent heat loss as a function of time from the skin for $M = 115$ W·m$^{-2}$ at $f = 25$, 45 and 60 rpm.

Table 2
Time-averaged mean of the steady periodic dry insulation and evaporative resistance values of the cotton-clothed walking human system current model

| Metabolic rate (W·m$^{-2}$) | $f$ (rpm) | $I_T$ (clo) | $R_{ET}$ (m$^2$·kPa·W$^{-1}$) |
|---|---|---|---|
| 115 | 25 | 0.97 | 0.0076 |
| | 45 | 0.725 | 0.0095 |
| | 60 | 0.645 | 0.0138 |
| 150 | 50 | 0.68 | 0.0085 |
| | 75 | 0.55 | 0.0067 |

evaporative resistance values from Eq. (22b) at $M = 115$ and 150 W·m$^{-2}$ are given in Table 2 at different ventilation frequencies. Both the dry insulation and evaporative resistance values decrease with increased ventilation frequency that corresponds to faster walking. Limited transient experimental data on walking clothed human are available that take into consideration the specific mechanism of ventilation with a light single layer of clothing. The current data

bases on standardized insulation measurements of separate garments or whole ensembles have been supplemented with results from movable thermal manikins. The theories still lag behind [19,27–30]. However, the presented results of insulation and evaporative resistance values will be compared qualitatively with published data Hong [19], Havenith et al. [27–29]. Published data of Hong on 24 different kinds of ensembles reports the dynamic insulation values at different walking speeds of selected indoor clothing ensembles using a movable thermal manikin [19]. Hong used the selected data to develop regression equations to predict the change in the insulation value due to body motion. Two of the reported experiments consider the case of a walking human (activity level is 2 Met = 115 $W{\cdot}m^{-2}$) wearing a long-sleeve sweat suit ensemble #17 (50% cotton, 50% polyester with fabric

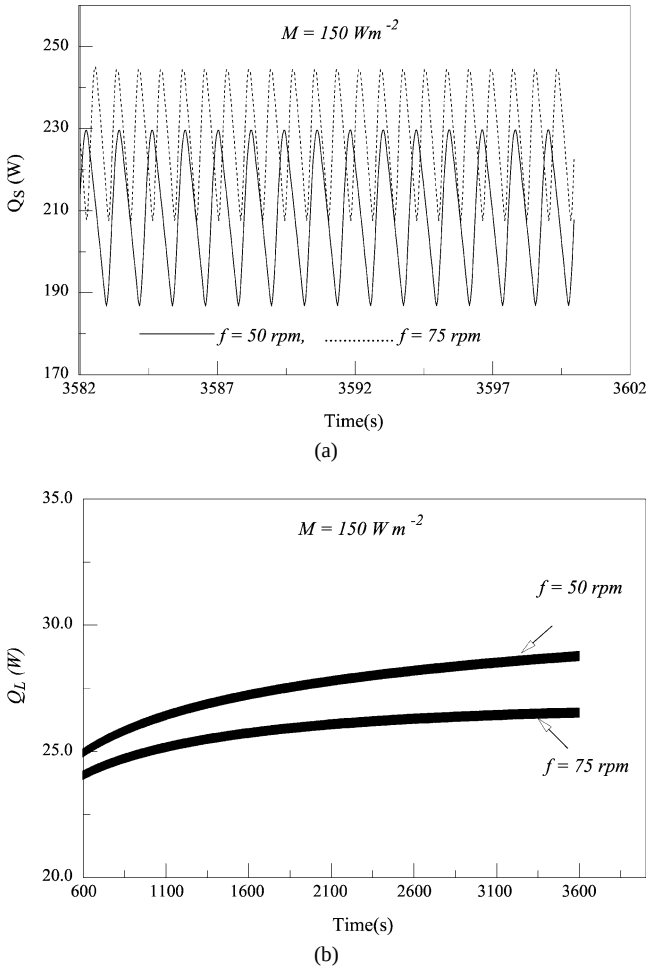


Fig. 8. (a) The predicted steady periodic sensible heat loss as a function of time from the skin for $M = 150$ $W{\cdot}m^{-2}$ at $f = 50$ and 75 rpm. (b) The predicted steady periodic latent heat loss as a function of time from the skin for $M = 150$ $W{\cdot}m^{-2}$ at $f = 50$ and 75 rpm.

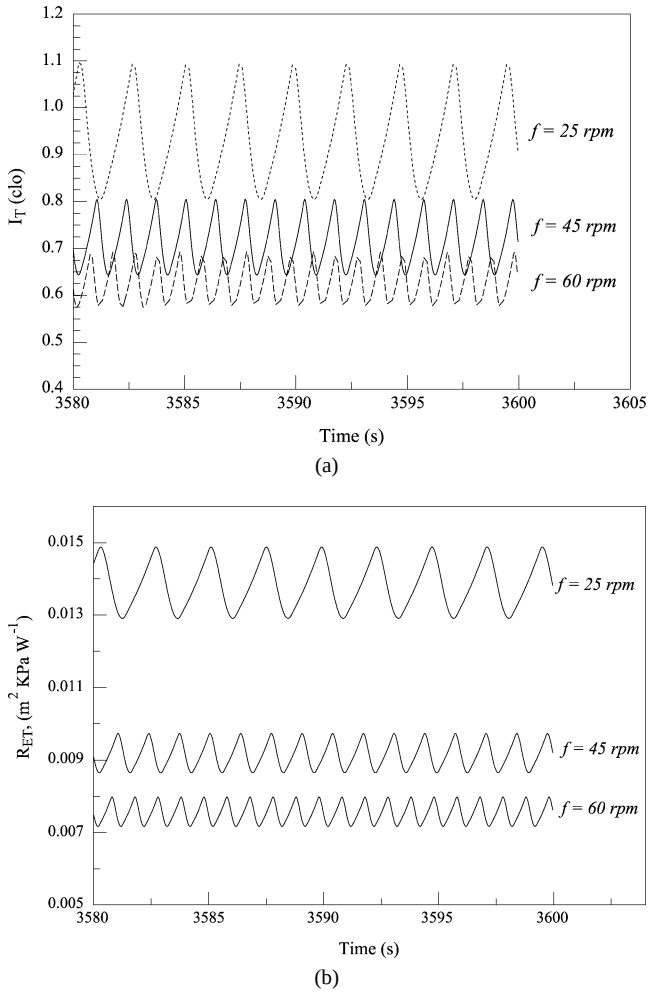


Fig. 9. (a) The predicted steady periodic dry insulation values as a function of time from the skin for $M = 115$ $W{\cdot}m^{-2}$ at $f = 25$, 45 and 60 rpm. (b) The predicted steady periodic evaporative resistance values as a function of time from the skin for $M = 115$ $W{\cdot}m^{-2}$ at $f = 25$, 45 and 60 rpm.

Table 3
Mean total dry insulation data ($I_T$) reported by Hong [19] and mean total insulation [27] and mean evaporative resistance [28] reported by Havenith et al.

| Data of Hong [19] | | | Data of Havenith et al. [27,29], ensemble A | | | |
|---|---|---|---|---|---|---|
| Ensemble number | Walking speed ($step{\cdot}min^{-1}$) | $I_T$ (clo) | Walking speed ($m{\cdot}s^{-1}$) | External wind ($m{\cdot}s^{-1}$) | $I_T$ (clo) Ref. [27] | $R_{ET}$ ($m^2{\cdot}kPa{\cdot}W^{-1}$) Ref. [28] |
| 4 | 0 | 1.45 | 0.3 | 0 | $1.05 \pm 0.1$ | $0.0316 \pm 0.001$ |
| 17 | 0 | 1.68 | | 0.7 | $0.91 \pm 0.08$ | $0.02107 \pm 0.001$ |
| | | | | 4.0 | $0.71 \pm 0.06$ | $0.00958 \pm 0014$ |
| 4 | 90 | 1.09 | 0.9 | 0 | $1.01 \pm 0.07$ | $0.02826 \pm 0.001$ |
| 17 | 90 | 1.05 | | 0.7 | $0.85 \pm 0.05$ | $0.0204 \pm 0.001$ |
| | | | | 4.0 | $0.57 \pm 0.03$ | $0.00838 \pm 0.0007$ |

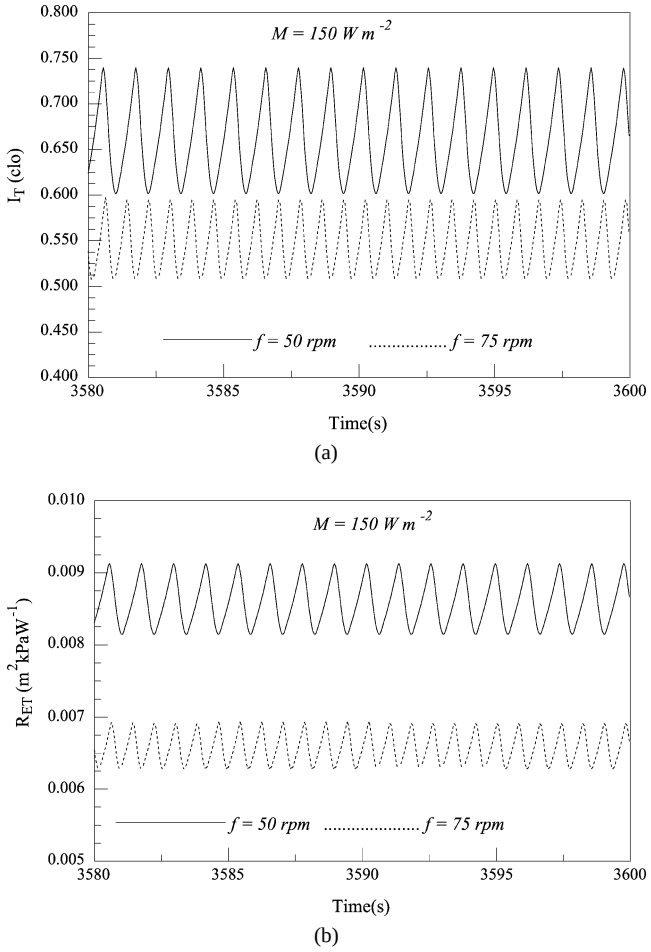


Fig. 10. (a) The predicted steady periodic dry insulation values as a function of time from the skin for $M = 150$ W·m$^{-2}$ at $f = 50$ and 75 rpm. (b) The predicted steady periodic evaporative resistance values as a function of time from the skin for $M = 150$ W·m$^{-2}$ at $f = 50$ and 75 rpm.

thickness of 3.9 mm) and the other wearing long sleeve turtle neck cotton sweater and cotton jeans #4. The environmental conditions of the experiments were at 22 °C, $RH = 50\%$. The measured standing and dynamic insulation values of ensemble 4 and 17 are presented in Table 2 showing a drop in the dynamic insulation from standing insulation values by 25 and 37%, respectively. For a clothing ensemble of cotton/polyester workpants, polo shirt, sweater, socks and running shoes, Havenith et al. published extensive data on mean total insulation values [27] and mean evaporative resistance values [28] for walking clothed human. Their data are given in Table 3 for walking speeds of 0.3 and 0.9 m·s$^{-1}$. The calculated dry total insulation values in the present work fall very close to the published data range on dynamic clothing insulation under walking conditions [19,27]. Evaporative resistances data in the present work fall slightly below the data of Havenith et al. [28,29], but are of the same order. Evaporative resistance comparisons and validations of results from water vapor resistance measurements often involve interpretation problems due to the lack of standardized measuring techniques and the strong dependence of the transport of vapor through the fabric material on fabric properties. While the current presented model has limitations, it does capture the complex mechanism of heat and moisture transport due to walking from applying the first principles of conservation of mass and heat on the combined human-clothing system. The limitations of the model can be relaxed by considering other factors that include the effect of the unexposed areas of the body and the 2-D convection inside the trapped air layer.

## 6. Conclusion

A thermal model of a walking clothed human was developed in this work by combining the human two-node model of Gagge's [15] and the three-node model of Ghali et al. [12,13]. The model predicts the transient thermal responses of the human and clothing giving temperatures, sensible and latent heat losses. The model also predicts the dynamic average insulation values of the clothing system.

The model results were physically sound and consistent with reported experimental data. The body heat loss to the environment and the fabric regain increase with increased ventilation frequency at fixed metabolic rate.

The model is built from first principles of mass and energy conservation, and hence represents a powerful tool for accurately predicting dynamic response of clothing systems. Improvements can be added to the human model, by considering exposed surfaces, finding the relation between the ventilation frequencies and effective wind/walking speeds, obtaining actual ventilation coefficients for the different parts of the body, and accounting for the losses associated with the openings in the clothing systems that may bring in additional convection.

## Acknowledgements

The authors wish to thank the Institute of Environmental Research at Kansas State University for allowing the use of their facilities. The authors greatly acknowledge the support of the University Research Board of the American University of Beirut Grant DCU-148860-73117.

## References

[1] K.L. Harter, S.L. Spivak, T.L. Vigo, Applications of the trace gas technique in clothing comfort, Textile Res. J. 51 (1981) 345–355.
[2] W. Lotens, Heat transfer from humans wearing clothing, Doctoral Thesis, published by TNO Institute for perception, Soesterberg, The Netherlands, 1993, pp. 34–37.
[3] B. Farnworth, A numerical model of combined diffusion of heat and water vapor through clothing, Textile Res. J. 56 (1986) 653–655.
[4] B.W. Jones, Y. Ogawa, Transient interaction between the human and the thermal environment, ASHRAE Trans. 98 (1) (1993) 189–195.
[5] W.J. Mincowycz, A. Haji-Shikh, K. Vafai, On departure from local thermal equilibrium in porous media due to a rapidly changing heat source: the Sparrow number, Internat. J. Heat Mass Trans. 42 (1999) 3373–3385.

[6] P. Gibson, Governing equations for multiphase heat and mass transfer in hygroscopic porous media with applications to clothing materials, Technical Report NATICK/TR-95/004 by United States Army Natick Research, December 1996, pp. 105 and 115–117.
[7] P. Gibson, K. Kendrick, D. Rivin, L. Sicuranza, M. Charmichi, An automated water vapor diffusion test method for fabrics, laminates and films, J. Coated Fabrics 24 (1995) 55–61.
[8] P. Gibson, M. Charmichi, Convective and diffusive energy and mass transfer in hygroscopic porous textile materials, in: Proceedings of the 1996 International Congress & Exposition, the ASME Winter Annual Meeting, No. 96-WA/HT-27, Atlanta, GA, November 1996, pp. 17–22.
[9] P. Gibson, M. Charmichi, The use of volume-averaging techniques to predict temperature transients due to water vapor sorption in hygroscopic porous polymer materials, J. Appl. Polymer Sci. 64 (1997) 493–505.
[10] P. Gibson, M. Charmichi, Coupled heat and mass transfer through hygroscopic porous materials – application to clothing layers, J. Soc. Fiber Sci. Technol. 35 (1997) 183–194.
[11] S. Whitaker, A Theory of Drying in Porous Media, in Advances in Heat Transfer, Academic Press, New York, 1977.
[12] K. Ghali, N. Ghaddar, B. Jones, Study of convective heat and moisture transport within porous cotton fibrous medium, 33rd ASME National Heat Transfer Conference, Paper No. NHTC2000-12072, Pittsburgh, USA, 2000.
[13] K. Ghali, N. Ghaddar, B. Jones, Multi-layer three-node model of convective transport within cotton fibrous medium, J. Porous Media 5 (1) (2002) 17–31.
[14] L. Ghali, N. Ghaddar, B. Jones, N. Awar, Modeling of heat and moisture transport by periodic ventilation of cotton Fibrous media, ASME 35th National Heat Transfer Conference, Anaheim, California, Paper No. NHTC2001-20175, 2001.
[15] A.P. Gagge, A. Fobelets, L.G. Berglund, A standard predictive index of human response to the thermal environment, ASHRAE Trans. 92 (2B), Paper No. PO-86-14, 1986.
[16] B.W. Jones, M. Ito, E.A. McCullough, Transient thermal response systems, in: Proceedings of the International Conference on Environmental Ergonomics, Austin, TX, 1990, pp. 66–67.
[17] Y. Li, B.V. Holcombe, Mathematical simulation of heat and moisture transfer in a human-clothing-environment system, Textile Res. J. 68 (6) (1998) 389–397.
[18] E.A. McCullough, B.W. Jones, T. Tamura, A data base for determining the evaporative resistance of clothing, ASHRAE Trans. 95 (2) (1989) 316–328.
[19] S. Hong, A database for determining the effect of walking on clothing insulation, Ph.D. Thesis, Kansas State University, Manhattan, Kansas, 1993.
[20] B.W. Jones, S. Hong, E.A. McCullough, Detailed projected area data for the human body, ASHRAE Trans. 104 (1998) 791–805.
[21] U. Danielsson, Convection coefficients in clothing air layers, Doctoral Thesis, The Royal Institute of Technology, Stockholm, 1993.
[22] J.R. Breckenridge, R.F. Goldman, Effect of clothing on bodily resistance against meteorological stimuli, in: J.F. Tromp (Ed.), Progress in Human Biometeorology, Swets en Zeitlinger, Amsterdam, 1977, pp. 194–208.
[23] X. Berger, The pumping effect of clothing, Internat. J. Ambient Energy 9 (1988) 37–46.
[24] J.J. Vogt, J.P. Meyer, V. Candas, J.P. Libert, J.C. Sagot, Pumping effect on thermal insulation of clothing worn by human subjects, Ergonomics 26 (1983) 963–974.
[25] E. McCullough, C. Kim, Insulation values for cold weather clothing under static and dynamic conditions, in: Y. Shapiro, D. Moran, Y. Epsen (Eds.), Environmental Ergonomic—Recent Progress and New Frontiers, Freund Publishing House, London, 1996, pp. 271–274.
[26] I. Holmer, H. Nilsson, G. Havenith, K. Parsons, Clothing convective heat exchange—proposal for improved predictions in standards and models, Ann. Occupat. Hygiene 43 (5) (1999) 329–337.
[27] G. Havenith, R. Heus, W.A. Lotens, Resultant clothing insulation: A function of body movement, posture, wind clothing fit and ensemble thickness, Ergonomics 33 (1) (1990) 67–84.
[28] G. Havenith, R. Heus, W.A. Lotens, Clothing ventilation, vapour resistance and permeability index: changes due to posture, movement and wind, Ergonomics 33 (8) (1990) 989–1005.
[29] G. Havenith, I. Holmer, E.A. Den Hartog, Clothing evaporative resistance—proposal for improved representation in standards and models, Ann. Occupat. Hygiene 43 (5) (1999) 339–346.
[30] A.C. Burton, O.G. Edholm, Man in Cold Environment, Edward Arnold, London, 1955.
[31] X. Berger, H. Sari, A new dynamic clothing model, Part 1: Heat and mass transfers, Internat. J. Thermal Sci. 39 (2000) 673–683.
[32] D.McK. Kerslake, The Stress of Hot Environments, Cambridge University Press, Cambridge, 1972.
[33] T. Mochida, Convective and radiative heat transfer coefficients for the human body, Bull. Faculty Engrg., Hokkaido University, 1970, pp. 1–11.
[34] ASHRAE, Handbook of Fundamentals, American Society of Heating, Refrigerating and Air Conditioning Engineers, Atlanta, 1993.
[35] W.E. Morton, L.W. Hearle, Physical Properties of Textile Fibers, Heinemann, London, 1975.
[36] B.W. Jones, Accurate modeling of heat and mass transport from the human body, in: AIAA 33rd Thermophysics Conference, Norfolk, VA, Paper No. AIAA-99-3500, 1999.
[37] P.O. Fanger, Thermal Comfort: Analysis and Application in Engineering, McGraw-Hill, New York, 1972.
[38] L.G. Berglund, A theoretical and experimental study of the thermoregulatory effects of salt accumulation on human skin during seating, Ph.D Thesis, Kansas State University, Manhattan, Kansas, 1971.
[39] R.W. Hyland, A. Wexler, Formulations for the thermodynamic properties of the saturated phases of $H_2O$ from 173.15 to 473.15 K, ASHRAE Trans. 89 (2A) (1983) 500–519.
[40] B.W. Jones, E.A. McCullough, Computer modeling for estimation of clothing insulation, in: Proceedings of the CLIMA 2000, World Congress on Heating, Ventilating and Air Conditioning, Copenhagen, Denmark, Vol. 4, 1985, pp. 1–5.